Soft Matter

Induction of entropic segregation: the first step is the hardest

SCHOLARONE™
Manuscripts

ARTICLE TYPE

Induction of entropic segregation: the first step is the hardest

Elena Minina[*] **and Axel Arnold**[*]

In confinement, overlapping polymers experience entropic segregating forces that tend to demix them. This plays a role during cell replication, where it facilitates the segregation of the daughter chromosomes. It has been argued that these forces are strong enough to explain chromosome segregation in elongated bacteria such as E. coli without the need for additional active mechanisms [S.Jun and B.Mulder, PNAS, 2006, **103**, 12388]. However, entropic segregation can only set in after the initial symmetry has been broken. We demonstrate that the timescale for this induction phase is exponentially growing in the chain length, while the actual segregation time scales only quadratically in the chain length. Thus the induction quickly becomes the dominating, slow process, and makes entropic segregation much less efficient than previously thought. The slow induction might also explain the long delay in chromosome segregation observed in experiments on E. coli.

1 Introduction

It is long known that polymers in confined geometries behave very differently from free polymer chains[1–3]. Their static properties and dynamics play an important role for example in DNA translocation through nanopores[4], chromosome organization[5–8], inkjet nozzles or polymers in nanofluidic devices[9]. The arguably most striking feature of confinement is the tendency of polymers chains to segregate for purely entropic reasons[10,11]. This means, that in an elongated cell such as an E. coli bacterium, two overlapping DNA molecules will move spontaneously to opposite ends of the cell even in the absence of active mechanisms[7,11,12]. It is still under debate whether this is the only mechanism responsible for DNA segregation during cell division, or whether additional active mechanisms are present as is the case in eukaryotic cells[6,13,14]. However, in order to distinguish the inevitable entropic segregation from possible active mechanisms, we need to understand its underlying mechanisms and timescales. This is a classical polymer problem in confined spaces, but has only recently attracted attention[7,15–17].

Theoretically, such systems can be tackled by de Gennes' blob model[1], which represents the polymer as a chain of blobs. Inside such a blob, the polymer is assumed to behave like a free polymer, unperturbed by constraints or other external forces. In the case of cylindrical confinement, the diameter of such a blob is determined by the cylinder diameter D. Using the fact that the cost for the overlap of two blobs is independent of chain length and small[18], it can be shown for example that the timescale for the segregation of two overlapping flex-

[*] Institute for Computational Physics, University of Stuttgart, Allmandring 3, 70569 Stuttgart, Germany. Fax: +49 711 6856 3658; Tel: +49 711 6856 3643; E-mail: minina@icp.uni-stuttgart.de

ible polymers in such confinement is $\mathscr{O}\left(N_t^2 D^{2-\frac{1}{\nu}}\right)$ with the Flory exponent $\nu \approx 0.6$ and N_t the total number of monomers in the polymer. Segregation times observed in computer simulations[7,11] agree well with this prediction. However, the simulations also show that the initial symmetry of the system has to be broken before the entropic segregation can set in. Before this has happened, two intially fully overlapping chains do not move with respect to each other, and no segregation can take place. Usually this induction phase takes a short period of time, but it might last even longer than the segregation process itself (compare also Fig. 4).

Such an induction phase is also observed in real bacteria. Experiments investigating cell division in E. coli show a delay of segregation after the initiation of the replication[6]. In these experiments, the origin of replication was traced by flourescent markers. Once the origin is replicated, the two sister origins should appear as two separate flourescent spots, which happens only 14 minutes after initiation of replication. During this time the origins remain colocalized and do not segregate.

In this article we investigate the origin of this induction phase. It was argued earlier that the symmetry breaking is a diffusive process with timescale $\mathscr{O}\left(N_t^3 D^{2-\frac{2}{\nu}}\right)$, that is, much slower than the actual segregation[11]. We will however show that the induction is in fact a rare event with an expontential timescale in the number of monomers.

The main mechanism of induction is not diffusion of the entire chains, but rather the arrangement of the chain ends. In order to start segregation, the two overlapping chains need to arrange such that different chains hang over at the two ends of the polymers (compare Fig. 1 (b)). In such a configuration, a small displacement of the size of a blob is sufficient to start segregation. If, however, one of the polymers is trapped
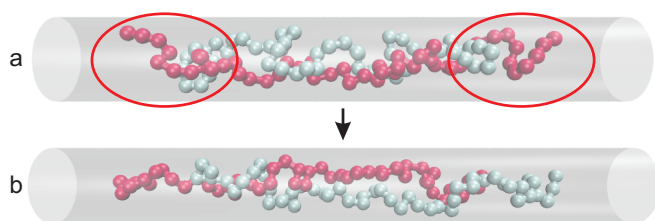
Fig. 1 Ordering of two polymers in a cylinder: (a) typical trapped polymer configuration during the induction phase; (b) configuration that allows for entropic segregation.
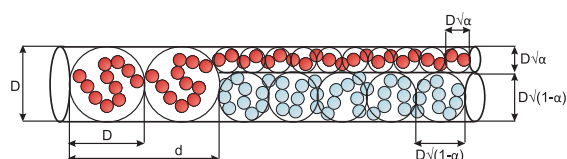

Fig. 2 Schematic view of an overhang configuration. The blob size is equal to the cylinder diameter D, the overhang is described by the difference d between the positions of the leftmost beads of the two chains. In the overlap region, we follow the model of Jung et al. [16] and assume the two chains to be confined to effective cylinders of diameter $D\sqrt{\alpha}$ and $D\sqrt{1-\alpha}$, respectively.

between the ends of the second one, segregation cannot start (Fig. 1 (a)). This trapping is the main origin of induction, and the timescale of induction is the timescale of the polymers switching roles at one of the ends.

This article is organized as following. In section 2 we use renormalized Flory theory [16] to compute the free energy barrier for switching of chain ends. The details of the molecular dynamics simulations are described in section 3. We conclude with results and discussions in section 4.

2 Theory

For simplicity, we consider only one half of the two polymers, that is, two overlapping self-avoiding linear polymers that consist of $N = N_t/2$ monomers of size a each and are confined in a cylinder of diameter D. Rather than enforcing full overlap, we allow the chains to partially segregate, however only at the one end of the two chains, compare Fig. 2. The other side corresponds to the center of the overlapping polymers. If the chains are sufficiently long, this is justified, because there is barely any interaction between the two ends. We use the difference d between the positions of the outermost beads of the chains to characterize the overhang. If $d = 0$, the chains are fully overlapping, however, we will show that this is typically entropically disfavored. Role switching of the chain ends is characterized by a sign switch of d. The timescale of this process is what we are interested in, since it characterizes the timescale to overcome a trapped configuration.

To determine the free energy of this system, we use the Flory free energy [19] of a single polymer of length N in a cylinder of diameter D. The polymer is represented as a chain of $n_{bl} = N/g$ blobs, where $g = (D/a)^{1/\nu}$ is the number of monomers per blob with $\nu \approx 0.6$. Inside such a blob, the polymer is considered to be a free self avoiding polymer with g monomers. The diameter of such a blob is the size of a free polymer coil of g beads, which by construction is D. Then the equilibrium length of the polymer is $L_{eq} = n_{bl}D$ and its free energy is [16,18]

$$\mathscr{F}(n_{bl}) = \mathscr{F}_{bl}n_{bl} = \mathscr{F}_{bl}N/g, \qquad (1)$$

where the constant $\mathscr{F}_{bl}$ is the free energy per blob, a non-universal constant depending on the type of polymer. Note that the diameter D enters the free energy only through the number of monomers in a blob, g.

The free energy of our system consists of three contributions: the first one is the free energy of the overhanging tail, the second and third contributions are the free energy of the remaining part of this polymer in the overlap region and the free energy of the other polymer, respectively. The free energy of the overhanging tail consisting of $n_0 = d/D$ overhanging blobs can be directly computed from the Flory energy and is

$$\mathscr{F}_1(n_o) = \mathscr{F}_{bl}n_o. \qquad (2)$$

To compute the free energy of the second and third contributions we extend the "renormalized" Flory approach proposed by Jung et al [16]. In this approach two fully overlapping polymers in a cylinder with diameter D are treated as two single polymers trapped in effective subcylinders of reduced diameter $D/\sqrt{2}$ each.

The overhanging polymer contributes less monomers to the overlap region than the trapped one, and thus occupies less space. This we model by considering two subcylinders with effective diameters $D_2 = D\sqrt{\alpha}$ and $D_3 = D\sqrt{(1-\alpha)}$, respectively, so that the parameter α is the area fraction of the cylinder occupied by the overhanging polymer in the overlapped region. Each subcylinder confines a single polymer that can be again considered as a sequence of blobs with a free energy given by Eqn. (1).

For the subcylinder of diameter D_2 the polymer splits into $(N - n_o g)/g_2$ blobs with $g_2 = (D_2/a)^{1/\nu} = g\alpha^{1/2\nu}$ monomers, so that its free energy is

$$F_2 = \mathscr{F}_{bl}(n_{bl} - n_o)\alpha^{-1/2\nu}. \qquad (3)$$

The trapped chain in the subcylinder of diameter D_3 has its full N beads in the overlap region and thus consists of N/g_3 blobs, where the number of monomers per blob is $g_3 = (D_3/a)^{1/\nu} = g(1-\alpha)^{1/2\nu}$. Its free energy is therefore

$$F_3 = \mathscr{F}_{bl}n_{bl}(1-\alpha)^{-1/2\nu}. \qquad (4)$$

Combining the three contributions, the free energy of the system with $n_o = |d|/D$ overhanging blobs is

$$\mathcal{F}(n_o, n_{bl}) = \mathcal{F}_{bl}\left[n_o + (n_{bl} - n_o)\alpha^{-1/2\nu} + \right.$$
$$\left. + n_{bl}(1-\alpha)^{-1/2\nu}\right]. \quad (5)$$

Again, the diameter D enters only indirectly through the number of monomers in a blob. The parameter α we determine from the condition that both chain segments in the overlap region should be in equilibrium and occupy the same stretch L along the cylinder:

$$L = (n_{bl} - n_o)D\sqrt{\alpha}^{1-1/\nu} = n_{bl}D\sqrt{1-\alpha}^{1-1/\nu}, \quad (6)$$

which leads to

$$\alpha(n_o, n_{bl}) = \left[1 + \left(1 - \frac{n_o}{n_{bl}}\right)^{2\nu/(\nu-1)}\right]^{-1}. \quad (7)$$

In the fully mixed state ($n_o = 0$) the splitting parameter is $\alpha = 1/2$, therefore the free energy of this state is

$$\mathcal{F}(n_o = 0, n_{bl}) = \mathcal{F}_{bl}n_{bl}2^{1+1/2\nu}. \quad (8)$$

We are left with determining the equilibrium number of overhanging blobs, n_o. To this aim, we insert the equilibrium splitting α in (5) and rewrite the free energy in terms of the ratio $\delta = n_o/n_{bl} = |d|/L_{eq}$. The free energy difference between configurations with overhang ratio δ given by Eqn. (5) and the fully mixed state $\delta = 0$ given by Eqn. (8) is

$$\frac{\Delta\mathcal{F}(\delta, n_{bl})}{n_{bl}\mathcal{F}_{bl}} = \frac{1}{n_{bl}\mathcal{F}_{bl}}[\mathcal{F}(\delta, n_{bl}) - \mathcal{F}(\delta = 0, n_{bl})] =$$
$$= \delta + (1-\delta)[(1-\delta)^{2\nu/(\nu-1)} + 1]^{1/2\nu} +$$
$$+ \left[(1-\delta)^{2\nu/(1-\nu)} + 1\right]^{1/2\nu} - 2^{1+1/2\nu}, \quad (9)$$

which solely depends on the ratio δ. Fig. 6 shows this universal free energy difference, which has a single, pronounced minimum, corresponding to the equilibrium state. We denote with $\mathcal{F}_{min}$ the free energy difference per blob between this minimum and the fully mixed state.

Note that our universal free energy curve predicts a nonzero gradient at $\delta = 0$. Therefore, the free energy as a function of the signed distance d has a sharp nondifferentiable peak at $d = 0$, which is clearly unphysical. This is due to the fact that the blob picture no longer holds for the overhanging part if $n_o \ll 1$, i.e. there are much less beads than necessary for a single blob. In that case, the overhanging part no longer feels the confinement, and thus has a different free energy with a smooth curvature. This is confirmed by our simulation data as presented below.
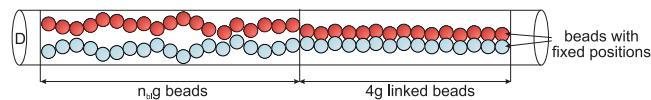

Fig. 3 Schematic view of the simulation setup. The two rightmost beads are fixed to prevent diffusion, the following $4g$ beads are pairwise crosslinked. Only the remaining $n_{bl}g$ beads on the left are free overlapping polymers.

When the polymers switch roles, i.e. when switching the sign of d, the free energy barrier $\mathcal{F}_{barrier} = n_{bl}\mathcal{F}_{min}$ between the minimum and $n_o = 0$ has to be overcome, making it a rare event. According to Kramer's or reaction-rate state theory[20] the switching rate k is

$$k \sim \mathcal{D}\sqrt{\mathcal{F}_0''\mathcal{F}_b''}e^{-\beta\mathcal{F}_{barrier}}, \quad (10)$$

where $\beta = 1/k_BT$ with the Boltzmann constant k_B and temperature T. $\mathcal{F}_0''$ and $\mathcal{F}_b''$ denote the curvatures at equilibrium distance and the top of the barrier, respectively. Following the scaling properties of the free energy, $\mathcal{F}_0''$ and $\mathcal{F}_b''$ scale like $1/(D^2n_{bl})$. Finally, $\mathcal{D}$ denotes the diffusion constant, which in our case is dominated by the motion of the outermost blob and therefore scales like $1/g$. Thus, the rate is

$$k \sim \frac{1}{D^2gn_{bl}}e^{-\beta\mathcal{F}_{barrier}} = \frac{1}{D^2N}\exp\left(-\beta\mathcal{F}_{min}\frac{N}{g}\right). \quad (11)$$

Coming back to the original question of the origin of the induction phase, we note that it is delayed whenever one of the polymers is trapped. To escape this trapping, the polymers have to switch roles at one of the two ends, and the induction time is nothing but the mean first passage time, which behaves like

$$t_{fs} \sim \frac{1}{k} \sim D^2N\exp\left(\beta\mathcal{F}_{min}\frac{N}{g}\right) \sim D^2N_t\exp\left(\beta\mathcal{F}_{min}\frac{N_t}{2g}\right), \quad (12)$$

in terms of the total length N_t of the two polymers. Note that there are only two non-universal parameters, namely the free energy minimum per blob $\mathcal{F}_{min}$, which captures the static properties of the polymer, and the proportionality prefactor, which captures its diffusional dynamics.

The most striking feature of Eqn. (12) is the exponential dependency on the number of monomers, in contrast to the earlier prediction $t_{fs} \sim N_t^3$ based on diffusion of the full chains[11]. We will now present computer simulation results that in depth verify the main assumptions in this derivation and show that Eq.(12) explains the induction time reported in Ref.[11] well.

3   Simulation method

Our simulations follow the approach used by Arnold and Jun in Ref.[11]. The cell membrane is represented as an open cylin-

der with diameter D, which mimics its growth during the cell cycle. We represent the polymers as a bead-spring chains of $N = N_t/2$ beads with diameter a, linked by spring-like bonds. The excluded volume of the beads as well as the wall are modeled by the Weeks-Chandler-Andersen (WCA) potential[21]:

$$U_{WCA}(r) = k_B T \begin{cases} \left(\frac{a}{r}\right)^{12} - \left(\frac{a}{r}\right)^{6} + \frac{1}{4} & r < \sqrt[6]{2}a \\ 0 & r \geq \sqrt[6]{2}a, \end{cases} \quad (13)$$

where r is the distance between two bead centers. The springs between the beads of the chains are finite extensible nonlinear elastic (FENE) bonds:

$$U_{FENE}(r) = -\frac{1}{2}\varepsilon_F \ln\left[1 - \left(\frac{r}{r_F}\right)^2\right], \quad (14)$$

where $r_F = 2a$ is the maximal stretch of the bond and $\varepsilon_F = 40 k_B T$ is the interaction strength. Note that ε_F is the product of the spring constant $10 k_B T/a^2$ and r_F^2, so that we employ the same FENE interaction as Ref.[11].

We perform molecular dynamics simulations of this system using the simulation package ESPResSo[22]. To propagate the system, we employ a velocity Verlet integrator[23] with a fixed time step of 0.01. The system is kept at constant temperature by means of a Langevin thermostat with dimensionless friction 1, which models embedding in a solvent.

For all graphs reported below, we use $v = 0.59$ as Flory exponent. In the simulations of the switching process, we recreate the system used for the theoretical considerations. We consider two polymers of length $(n_{bl} + 4)g$ with two beads on one end fixed, which prevents center of mass diffusion along the cylinder. The number of beads per blob was determined from fitting $g = (D/a)^{1/v}$ to the single chain data given in Ref.[24], from which we obtained $a = 1.31$. Initially, the system is prepared ladder-like, i.e. the ith beads of both polymers are bonded. After equilibration we remove $n_{bl}g$ crosslinking bonds, but keep four blobs next to the fixed beads interconnected (compare Fig. 3). These four blobs are used as a buffer to prevent back-bending of the polymers. We then vary the diameter of the cylinder $D = 3, 4, \ldots, 7$ and the non-crosslinked length of the polymers $N = n_{bl}g$, where $n_{bl} = 5, 6, \ldots, 20$. The resulting free chain lengths are between 30 and 550 beads. The scaling of the length with the diameter ensures that the polymers are neither too short at large diameters, nor excessively long at small diameters. We perform $500,000$ time steps for each parameter set.

4 Results

We start first with showing the distributions of induction and segregation time for segregation of two polymers with $N = 300$ beads each in cylinder of diameter 7 in Fig. 4. Unlike in
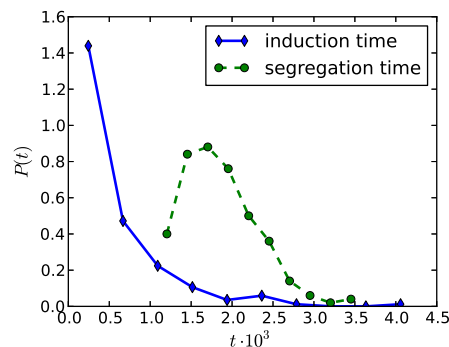

Fig. 4 Exemplary distribution of the induction and segregation time t obtained from computer simulations of polymers consisting of $N_t = 300$ beads each in a cylinder of diameter $D = 7$.
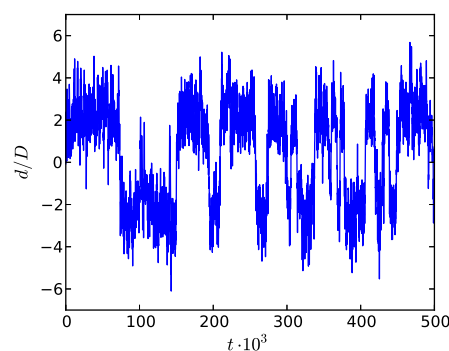

Fig. 5 Difference d between the positions of the leftmost beads versus time t for two polymers of length $n_{bl} = 10$ beads in a cylinder of diameter $D = 5$. A sign switch indicates that the overhanging polymer has switched.

what follows, the polymers are completely free to move, but are initially setup such that they fully overlap, following the procedure described in Ref.[11]. The distributions clearly differ, with the induction time being expontially distributed, as one would expected for the described switching mechanism. In this case of a relatively short chain, the mean induction time is still shorter than the mean segregation time, but already comparable. This shows that the induction phase is by no means negligible in the overall segregation process.

Fig. 5 shows the evolution of the difference d of the positions of the outermost free beads for an exemplary simulation with $n_{bl} = 10$ blobs in a cylinder of diameter $D = 5$. Sign switching of d indicates that the overhanging polymer has switched. Clearly, this switching is a rare event with a moderate barrier height. Fig. 5 also shows that the overhang is on average approximately 2 blobs. This reflects that the trapped polymer cannot be compressed too strongly, but on the other
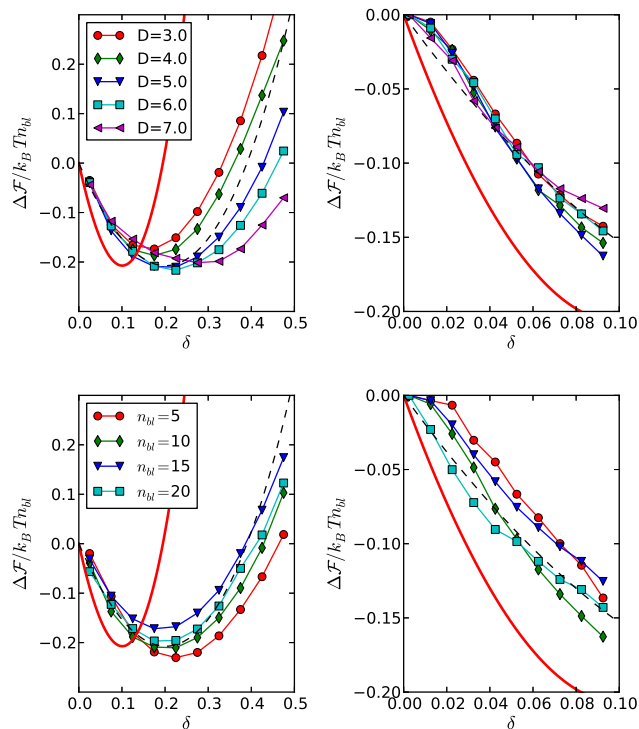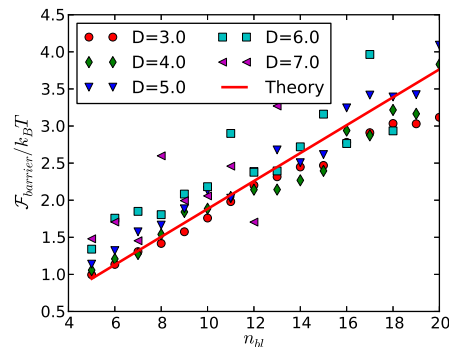
Fig. 7 The height of the energy barrier $\mathscr{F}_{barrier}$ as a function of the polymer length in terms of blobs $n_{bl} = N/g$ for various diameters D of the cylinder. The line is the theoretical prediction $\mathscr{F}_{min}n_{bl}$, using the free energy barrier per blob $\mathscr{F}_{min} \approx 0.19k_BT$ as single fit parameter for all curves.

Fig. 6 Free energy difference landscapes for fixed $n_{bl} = 10$ (top) and fixed $D = 5$ (bottom). The left graphs show free energies as measured in the simulations and our prediction Eqn. (9) (solid red) as a function of the ratio $\delta = n_o/n_{bl} = |d|/(Dn_{bl})$, assuming a free energy of $\mathscr{F}_{bl} = 5k_BT$ per blob. The dashed black line gives the same prediction using an effective overhang $\delta_{eff} = 0.5\delta$. The right graphs show the same data, but zoomed in at the top of the barrier. This demonstrates that the free energy difference is a smooth function at the top of the barrier $\delta = 0$.

hand, a fully mixed state is unfavorable, as predicted.

From the distribution of the number of overhanging blobs we can compute the free energy of a certain overhang by $\Delta\mathscr{F}(\delta)k_BT = -\ln P(\delta) + \ln P(0)$. Fig. 6 shows the free energy distribution for fixed diameter $D = 5$ and fixed $n_{bl} = 10$, respectively. We also show our free energy prediction Eqn. (9), where we have chosen as free energy per blob $\mathscr{F}_{bl} = 5k_BT$ to match our simulation results.

While the overall shape is well predicted by our theory, the equilibrium overhang is clearly underestimated. However, if we use and effective overhang of $\delta_{eff} = 0.5\delta$, we can match the simulation data rather well. This is probably due to the fact that the transition between overlap and overhang region is not sharp as in our model, but smoothed out, which effectively decreases the overhang. This assumption is supported by Fig. 6 of Ref. [24], which shows that the density of beads of the overlapping chains gradually changes along the cylinder

main axis.

Note that the collapse is much better for the constant diameter than constant number of blobs. This is due to the fact that the scaling regime is only realized for relatively large diameters as reported before [16,24]. However this would require longer polymers, which would make the sampling of the energy barrier problematic due to the large free energy difference. The right hand graphs of Fig.6 demonstrates that unlike our prediction, the free energy is not peaked at $\delta = 0$, but smooth. However, the curvature is surprisingly large, so that this curvature dominates the prefactor of the switching rate.

Fig. 7 shows the numerically determined depth of the minimum for a wide range of cylinder diameters and chain lengths. There is some spread in the data because the bottom of the free energy landscape is relatively flat and we report the numerically lowest observed free energy. Nevertheless, for all diameters D and chain lengths, we find the energy barrier to scale linearly with n_{bl} as predicted by Eq. (5), and by fitting to our results, we can determine that $\mathscr{F}_{min} \approx 0.19 \pm 0.05k_BT$ for our polymer model. This value we use in all remaining plots.

Fig. 8 shows that also the switching rate k scales like $k \sim \exp(-\beta\mathscr{F}_{min}n_{bl})/(D^2N)$ as predicted. To that aim we plot the rate of switching times D^2N versus the polymer length in terms of blobs. In the simulations, we measure the rate of switching by counting sign changes in d, however recording d only every 100 time steps to avoid counting recrossings. Again there is noticable spread in the data for larger diameters, because the rate decreases with the diameter, making it difficult to measure. However, the $D = 3$ curve clearly lies somewhat below the rest of the data, which we attribute to the fact that the blob picture does not hold well at these relatively small diameters. The data for $D > 4$ distributes around $k = \gamma/(D^2N)\exp(-\beta\mathscr{F}_{min}n_{bl})$, where we insert $\mathscr{F}_{min} = 0.19k_BT$
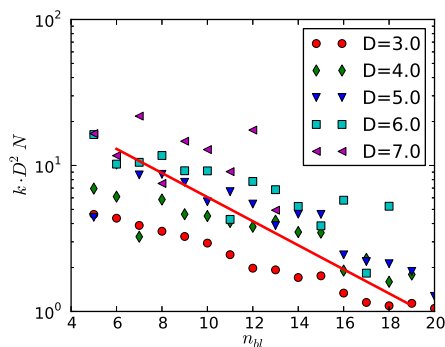
Fig. 8 The rate of switching k times D^2N versus the polymer length in terms of blobs $n_{bl} = N/g$. The solid line shows the predicted exponential scaling relation (11) using the previously measured $\mathscr{F}_{min} \approx 0.19k_BT$.

Fig. 9 The induction time t_{fs} as given in Ref.[11] rescaled by D^2N_t versus the number of blobs n_{bl} for different number of monomers N_t per chain. The data agree well with our theoretical prediction (12) for the induction time using the previously determined barrier per blob $\mathscr{F}_{min} = 0.19k_BT$, which is shown as red line. Above 20 blobs, the data still collapses, but deviates from the exponential prediction due to small cylinder diameters.

as determined from Fig. 7. The only remaining fitting parameter was the effective friction coefficient γ, which we found to be approximately 12 in dimensionless simulation units[11].

Finally, Fig. 9 shows that the induction time scales indeed like $1/k$, as predicted. In this figure, the data given in Fig. 5 of Ref.[11] was replotted not as a function of the diameter D, but as function of the total number of blobs. The induction time was rescaled by D^2N_t, so that Eqn. (12) predicts a single exponential increase, which is well reproduced by our data for n_{bl} up to 20. For larger n_{bl}, the data still collapses, but does not follow the predicted exponential. This is due to the fact that by construction of this data, the diameter decreases with increasing n_{bl}, and we reach the lower limit $D = 4$ for the blob picture to hold. Since the simulation models are identical, we employ the same barrier free energy per blob $\mathscr{F}_{min}$ in the slope of the exponential, which fits the data rather well. This is another strong indication that the role switching plays an important role for the induction phase.

5 Conclusions

We have investigated the induction phase of the segregation process of flexible chains in a confining cylinder. Our results suggest that the induction phase is not governed by diffusion of the chains as argued before, but rather by an ordering process at the polymer ends. It is entropically favorable for the polymers to at least partially segregate at their ends. As this happens independently, one polymer may be trapped by the other, so that no segregation can take place. This trapped state has to be overcome by switching the roles of the polymers on one side, which is a rare event due a free energy barrier at full overlap. Both free energy calculations based on the blob model and molecular dynamics simulations show that the
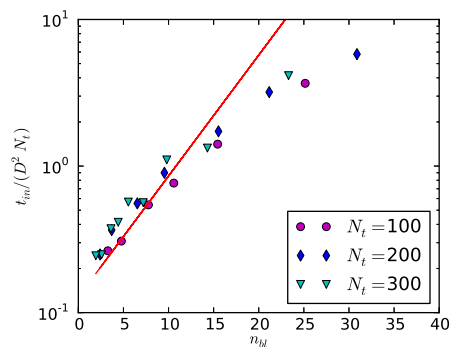
height of the barrier is proportional to the number of blobs in the polymer. Using Kramer's theory one can estimate the switching rate and by that the duration of the induction phase, which scales exponentially with the energy barrier und thus the length of a polymer. For long polymers, the induction time therefore becomes dominating over the actual segregation time, making entropic segregation a very slow process on average.

Acknowledgements

References

1 *Scaling Concepts in Polymer Physics*, ed. P.-G. de Gennes, Cornell University Press, London, 1st edn, 1979.

2 S. Daoudi and F. Brochard, *Macromolecules*, 1978, **11**, 751–758.

3 J. Kim, C. Jeon, H. Jeong, Y. Jung and B.-Y. Ha, *Soft Matter*, 2013, **9**, 6142–6150.

4 A. Meller, L. Nivon, E. Brandin, J. Golovchenko and D. Branton, *PNAS USA*, 2000, **97**, 1079–1084.

5 J. Kindt, S. Tzlil, A. Ben-Shaul and W. M. Gelbart, *Proceedings of the National Academy of Sciences*, 2001, **98**, 13671–13674.

6 D. Bates and N. Kleckner, *Cell*, 2005, **121**, 899–911.

7 S. Jun and B. Mulder, *Proceedings of the National Academy of Sciences*, 2006, **103**, 12388–12393.

8 S. De Nooijer, J. Wellink, B. Mulder and T. Bisseling, *Nucleic acids research*, 2009, **37**, 3558–3568.

9 J. O. Tegenfeldt, C. Prinz, H. Cao, S. Chou, W. W. Reisner, R. Riehn, Y. M. Wang, E. C. Cox, J. C. Sturm, P. Silberzan *et al.*, *Proceedings of the National Academy of Sciences of the United States of America*, 2004, **101**, 10979–10983.

10 S. Jun, A. Arnold and B.-Y. Ha, *Phys. Rev. Lett.*, 2007, **98**, 128303.

11 A. Arnold and S. Jun, *Phys. Rev. E*, 2007, **76**, 031901.

12 B. Youngren, H. J. Nielsen, S. Jun and S. Austin, *Genes & development*, 2014, **28**, 71–84.

13 K. Gerdes, J. Moller-Jensen, G. Ebersbach, T. Kruse and K. Nordström, *Cell*, 2004, **116**, 359 – 366.

14 Z. Gitai, *Cell*, 2005, **120**, 577 – 586.

15 J. Shin, A. G. Cherstvy and R. Metzler, *arXiv preprint arXiv:1401.5932*, 2014.

16 Y. Jung, C. Jeon, J. Kim, H. Jeong, S. Jun and B.-Y. Ha, *Soft Matter*, 2012, **8**, 2095–2102.

17 Y. Liu and B. Chakraborty, *Physical biology*, 2012, **9**, 066005.

18 A. Y. Grosberg, P. G. Khalatur and A. R. Khokhlov, *Die Makromolekulare Chemie, Rapid Communications*, 1982, **3**, 709–713.

19 S. Jun, D. Thirumalai and B.-Y. Ha, *Physical review letters*, 2008, **101**, 138101.

20 P. Hänggi, P. Talkner and M. Borkovec, *Rev. Mod. Phys.*, 1990, **62**, 251–341.

21 J. D. Weeks, D. Chandler and H. C. Andersen, *The Journal of Chemical Physics*, 1971, **54**, 5237–5247.

22 H. Limbach, A. Arnold, B. Mann and C. Holm, *Computer Physics Communications*, 2006, **174**, 704 – 727.

23 *Understanding Molecular Simulation. From Algorithms to Applications*, ed. D. Frenkel and B. Smit, Academic Press, 2nd edn, 2001.

24 A. Arnold, B. Bozorgui, D. Frenkel, B. Y. Ha and S. Jun, *Journal of Chemical Physics*, 2007, **127**, 164903.